

Using soft X-ray observations to help the prediction of flare related interplanetary shocks arrival times at the Earth

H.-L. Liu^{1,2} and G. Qin¹

Received 5 October 2011; revised 5 February 2012; accepted 13 March 2012; published 28 April 2012.

[1] It is very important to predict the shock arrival times (SATs) at Earth for space weather practice. In this paper we use the energy of soft X-ray during solar flare events to help predict the SATs at Earth. We combine the soft X-ray energy and SAT prediction models previously developed by researchers to obtain two new methods. By testing the methods with the total of 585 solar flare events following the generation of a metric type II radio burst during the Solar Cycle 23 from September 1997 to December 2006, we find that the predictions of SATs at Earth could be improved by significantly increasing POD_n , the proportion of events without shock detection that were correctly forecast. POD_n represents a method's ability in forecasting the solar flare events without shocks arriving at the Earth, which is important for operational predictions.

Citation: Liu, H.-L., and G. Qin (2012), Using soft X-ray observations to help the prediction of flare related interplanetary shocks arrival times at the Earth, *J. Geophys. Res.*, 117, A04108, doi:10.1029/2011JA017220.

1. Introduction

[2] The interplanetary (IP) shocks can bring changes to the terrestrial environment which, together with other space weather phenomena, might be able to damage the performance of space-borne and ground-based electronic technology systems. So it's very essential to build operational prediction models, based on very early solar (or near-sun) diagnostics, that can provide whether the shocks will arrive at the Earth, and the shock arrival times (SATs) and strength if they will.

[3] Some physics-based models have been developed, such as the Shock Time of Arrival (STOA) model [Dryer and Smart, 1984; Smart *et al.*, 1984, 1986; Smart and Shea, 1985; Lewis and Dryer, 1987], the Interplanetary Shock Propagation Model (ISPM) [Smith and Dryer, 1990] and the Hakamada-Akasofu-Fry/version-2 (HAFV.2) model [Fry *et al.*, 2001]. All the three models use similar observational data as inputs which include flare's solar longitude, start time of the metric type II radio drift, the proxy piston-driving time duration and solar wind speed. The STOA is an empirical model. In our new method of predicting the SATs, we use this model to give the specific arrival times of the IP shocks when Yes predictions are given. In STOA model the

initial explosion, flare, not the CME drives the IP shock, and after the driven stage, the shock will decelerate as a blast wave. The blast wave rides over a uniform background solar wind. The HAFV.2 model is a kinematic model which can be used to study the propagation of the interplanetary disturbances. Compared with previous models such as STOA and their improved SEP additions, the more sophisticated 3D MHD models [Odstrcil *et al.*, 2002; C. C. Wu *et al.*, 2006; Detman *et al.*, 2006; Feng *et al.*, 2007] address the background plasma and IMF inhomogeneity, e.g., CIRs, sector boundaries, etc.

[4] In addition, Feng *et al.* [2009] developed a database method for prediction of SATs at Earth by creating databases using previous numerical prediction models that include the influence of the initial shock speed and source longitude's impact.

[5] Some characteristic speed of CME were also used to help predicting the SATs of IP shocks [Manoharan *et al.*, 2004; Schwenn *et al.*, 2005; Gopalswamy *et al.*, 2005]. IP shocks driven by CMEs will arrive earlier than the CMEs, and the time difference between them depend on the geometry of the driving CME and the upstream Alfvénic Mach number. Sometimes a corresponding ICME couldn't be detected at L1 due to the interaction with the ambient solar wind. In this paper we will only focus on the shocks related with solar flares following the metric type II radio bursts during Solar Cycle 23.

[6] Much work has been done to test the performance of the SAT prediction models [e.g., Smith *et al.*, 2000, 2004, 2009a; Fry *et al.*, 2003; McKenna-Lawlor *et al.*, 2006]. Standard meteorological methodology could be adopted to analysis the predictions and observations using shock events observed during Solar Cycle 23. [McKenna-Lawlor *et al.*, 2006]. Our work also use these method and data to test the two new methods.

¹State Key Laboratory of Space Weather, Center for Space Science and Applied Research, Chinese Academy of Sciences, Beijing, China.

²College of Earth Sciences, Graduate University of Chinese Academy of Sciences, Beijing, China.

Corresponding Author: H.-L. Liu, State Key Laboratory of Space Weather, Center for Space Science and Applied Research, Chinese Academy of Sciences, PO Box 8701, Beijing 100190, China. (hlliu@spaceweather.ac.cn)

Copyright 2012 by the American Geophysical Union.
0148-0227/12/2011JA017220

[7] IP shocks are not the only products of solar flares, which also release some electromagnetic and particle radiation. SEPs move much faster than the shocks associated with them, so SEPs may be used to help predicting the SATs. Based on this point of view, *Qin et al.* [2009] presented a SAT prediction model STOASEP by combining the observation of the high energy solar energetic electrons at L1 with the well-known prediction model STOA. The STOASEP model remarkably improves the ratio of the correct predictions to false alarms. Like the SEPs, soft X-rays and radio bursts are also related to flares and shocks closely and might be used to help predicting SATs too. Dryer proposed that soft X-ray and metric radio drifts [e.g., *Smerd, 1970; Stewart et al., 1970; Dulk et al., 1971*] be used as he described in various papers and reviews for a reasonably high probability warning [e.g., *Dryer, 1974*]. It is known that the peak intensities of soft X-rays are used to classify the solar flare events. *Smith et al.* [1994] discussed the probability of soft X-ray as a proxy for total energy injected by a flare into the interplanetary medium (E). The total energy was estimated from observed coronal shock velocities, source duration, and spatial extent using an empirical equation. The integral under the curve between the flare's start and stop times was used as the energy released by the flare in soft X-ray (E_x). Although, it was claimed that E_x couldn't be used as a proxy for the total flare energy into the IP medium, E , but at least the two of them are correlated [*Smith et al., 1994*]. In addition, the soft X-rays could be observed much earlier than the IP shocks associated with the same flare. Therefore, it's possible to improve the real-time predictions of SATs with the help of E_x from the soft X-ray observations.

[8] In this paper, we study the prediction of SATs with the help of soft X-ray observations. We briefly describe the STOA and STOASEP models developed previously by researchers in section 2. In section 3, we present two new SAT prediction methods by combining STOA and STOASEP models with the analysis of soft X-ray observations. We study the performance of different models in section 4. In section 5, we present conclusions and discussions.

2. Description of STOA and STOASEP Models

[9] The Shock Time of Arrival (STOA) model [*Smart and Shea, 1985*] is widely used to predict shocks arrival times. It is based on the similarity theory of blast waves, modified by the piston-driving concept, that emanate from point explosion. STOA model divides the propagation of an IP shock into two stages. In the first stage, the shock is initially driven at a constant speed which is derived from the metric type II radio frequency drift rate. Then the shock entered the second stage, the blast wave phase, in which the blast wave rides over a uniform background solar wind. In this model the magnetoacoustic Mach number is used to measure the strength of the shock, and $M_a = 1.0$ is a limit below which shocks decay to MHD waves. Besides other references, *Qin et al.* [2009] could also be referred for the details of STOA model.

[10] *Qin et al.* [2009] developed a new SAT prediction model, STOASEP, by combining the STOA model with the help of the high energy solar energetic electron measurements (0.038–0.053 MeV, 5-minute averaged level two data

of ACE/EPAM). In their model they use the shock strength limit, $M_a = 1.0$ (like in STOA model), and the ratio (R) of the target flux (F_t) to the background flux (F_b) to decide whether the shock could arrive at the Earth. Here the 10-minute averaged energetic electron flux during the time range [$t_{SE} + 142.5 \text{ min} : t_{SE} + 152.5 \text{ min}$] is taken as the F_t , with t_{SE} the solar event time, and F_b is the 30-minute averaged flux during the time range [$t_{SE} - 15 \text{ min} : t_{SE} + 15 \text{ min}$]. The STOASEP model uses a threshold of ratio $R_t = 1.05$. If $M_a > 2$, STOASEP will make a “Yes” prediction; If $M_a \leq 1$, a “No” prediction will be made by the model; when $1 < M_a < 2$, the model STOASEP will make a prediction depending on the ratio R , if $R > R_t$ or $R \leq R_t$, a “Yes” or “No”, respectively, prediction will be made. Furthermore, the STOASEP model uses STOA model to predict the shock arrival time if it is predicted that the shock would arrive.

3. Predicting the SATs With the Help of Energy Released by Flare in Soft X-Rays, New Methods STOAF and STOASF

[11] There are 622 solar flare events following the generation of type II radio burst in the Solar Cycle 23 covering the period from 4 September 1997 to 14 December 2006, in which 170 events during the rise phase were compiled by *Fry et al.* [2003], 207 events during the maximum phase were compiled by *McKenna-Lawlor et al.* [2006], and 245 events during the decline phase were compiled by *Smith et al.* [2009b]. We try to use soft X-ray energy to improve SAT prediction. However, in *Fry et al.* [2003] the soft X-ray peak intensity data for the flare events are not given, but they are available online at <http://www.ngdc.noaa.gov/stp/solar/solardataservices.html>. When matching the soft X-ray peak intensity data with flare events in the rise phase, the data of the nearest event in time is used. In addition, there are 37 of the total 622 events removed because of the lack of soft X-ray intensity data, so in this work we only use the left 585 solar flare events.

[12] Figure 1 shows scattered plot of the peak intensity of soft X-ray (f) against the duration of the flare event (τ) of the 585 solar flare events during Solar Cycle 23 covered from September 1997 to December 2006. In the figure the red triangles indicate that the flare events are accompanied by shocks at L1, and the green triangles indicate that the flare events are not accompanied by shocks at L1. From Figure 1 we can see, in Region I when the soft X-ray peak intensity f or the duration of the flare event τ are small enough, almost all the triangles are green, which means that the flare events with weak soft X-ray can not generate shocks arriving at the Earth. On the other hand, most of the events located in Region III of the figure are accompanied by shocks detected at L1, so the triangles there are almost all red. Region III stands for strong X-ray peak intensity and long duration of flare events. For events with moderate intensity and duration in Region II of the figure, the triangles with different color are more equally distributed in f and τ space than that in the other two regions.

[13] *Smith et al.* [1994] studied the relationship between the total energy released from the Sun in a flare event E and the energy in soft X-ray E_x . They gave the definition of E_x , integrating under the curve between the flare's start and stop

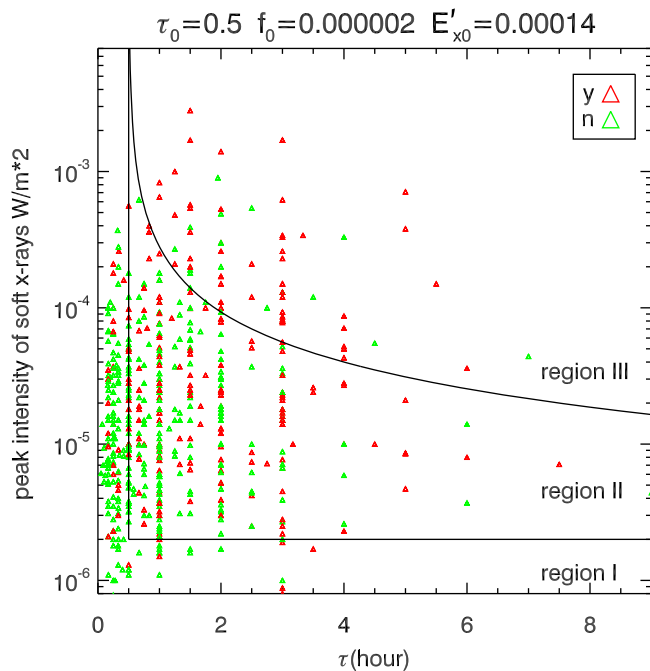


Figure 1. The peak intensity of soft X-ray (f) against the duration of the flare event (τ) of the 585 solar flare events during Solar Cycle 23 covered from September 1997 to December 2006. Red triangles indicate that the flare events are accompanied by shocks at L1, and the green triangles indicate that the flare events are not accompanied by shocks at L1.

time. To get a finite area for integrating, a baseline at one-half of the maximum flux was selected. The type II start time was regarded as the start time of the events. Based on the definition of E_x in *Smith et al.* [1994], we define a simplified variable E'_x from the soft X-ray peak intensity f and the duration time τ to approximately measure the strength of an X-ray event as,

$$E'_x = (f - f_0)(\tau - \tau_0), \quad (1)$$

where the threshold soft X-ray peak intensity f_0 and threshold duration time τ_0 are set as 2×10^{-6} W/m² and 0.5 hr, respectively, to make our new prediction methods below the best. Note that when the soft X-ray peak intensity $f \gg f_0$ and the duration time $\tau \gg \tau_0$, the simplified variable E'_x is in the order of soft X-ray energy E_x .

[14] In our new methods if the soft X-ray peak intensity or the duration time is not larger than the threshold values, we predict there is no shock arrival at the Earth because of the too weak X-ray event. Otherwise, if the E'_x is larger than a threshold value $E'_{x0} = 0.00014$ Whr/m² we predict there is

shock arrival at the Earth because of the strong X-ray event. For the rest of cases with moderate X-ray events we use STOA model or STOASEP model to predict whether the shock would arrive at the Earth. Note that similar as *Qin et al.* [2009] in STOASEP we use 5-minute averaged solar energetic electron measures from the DE1 channel of ACE/EPAM level two data with energy range 0.038–0.053 MeV [Gold et al., 1998]. For any event if the shock is predicted to arrive at the Earth, we use STOA to further predict the time when the shock will arrive. The new method that combine the soft X-ray observations and the STOA model to predict if the shock will arrive is called STOAF, while the other one that combine the soft X-ray observations and the STOASEP model is called STOASF.

4. Performance of New Methods, STOAF and STOASF

[15] A standard meteorology methodology can be used to test a forecast model. It is known that there are four possible results for one prediction, hit (h), miss (m), false alarm (fa) and correct null (cn). If the model makes a Yes prediction and a shock is detected within ± 24 hours of the predicted time the result is “hit”. On the other hand, if a shock is detected but none is predicted or the predicted time given by the model is more than 24 hours before or after the detection, it is “miss”. Furthermore, “false alarm” refers to a shock predicted but none is observed within a window of one to five days following the solar flare event. While “correct null” means that no shock is predicted and none is observed within four days after the solar flare event. Note that “hit” + “miss” represents the number of observed events with shock and that “false alarm” + “correct null” represents the number of events without shock. Table 1 shows the performance of STOA, STOASEP, STOAF, and STOASF evaluated with the 585 solar flare events in Solar Cycle 23 described in section 1. Columns 4–7 of Table 1 show the contingency entries. Column 8 lists the ratios of hit/miss (h/m). Column 9 shows the success rates (sr) which is defined as $(h + cn)/(h + m + fa + cn)$. A χ^2 test is used to indicate the dependency between the IP shocks’ observations at L1 and the predictions given by these methods. A significance level of 0.05 is adopted here. Larger χ^2 value means that the dependence between the observations and the predictions is better. P-value indicates the statistical significance of the forecasts. And $p < 0.05$ indicates a high level of significance. The statistical significance of the prediction results is indicated by χ^2 and p-values listed in column 10 and column 11.

[16] Since sometimes it is not very clear which event matches with a certain shock, especially when multiple events are very near in time, for a model we can re-arrange the event-shock pairs within a narrow range to get the best performance in statistics. Here, to check the performance of

Table 1. Comparison of the Results Obtained Using Different Models for Samples During Solar Cycle 23^a

Status	Number of Events	Model	(h)	(fa)	(cn)	(m)	(h/m)	(sr)	χ^2	p-Value
Cycle 23	585	STOA	174	230	126	55	3.1	0.51	8.44	0.003
		STOASEP	154	158	198	75	2.1	0.60	29.2	< 0.0001
		STOAF	157	149	207	72	2.2	0.63	39.8	< 0.0001
		STOASF	144	112	244	85	1.7	0.66	55.9	< 0.0001

^aHit window size ± 24 hours.

Table 2. Statistical Comparison of the Performances of STOA, STOASEP, STOAF and STOASF in Terms of Several Standard Meteorological Forecast Skill Scores Using the 622 Events During Solar Cycle 23 Selected for Table 1

	STOA	STOASEP	STOAF	STOASF
Probability of detection, yes (POD _y)	0.75	0.67	0.68	0.63
Probability of detection, no (POD _n)	0.35	0.55	0.58	0.68
False alarm ratio (FAR)	0.56	0.50	0.48	0.43
BIAS	1.76	1.36	1.33	1.11
Critical success index (CSI)	0.37	0.39	0.41	0.42
True skill statistic (TSS)	0.11	0.22	0.26	0.31
Heidke skill score (HSS)	0.10	0.21	0.25	0.30
Gilbert skill score (GSS)	0.05	0.12	0.14	0.18
Root mean square of ΔT , hours	11.6	11.5	11.9	11.5
Success Rate (sr)	0.51	0.60	0.62	0.66

different models we use the event-shock pairs best for the STOA model. It is possible we could improve any other models' performance in statistics a little by re-arranging the event-shock pairs within a narrow range. However, the overall results are not changed.

[17] We can see from Table 1 that STOA model gives the highest value of hit, but also the highest false alarm. Generally speaking, STOA model tends to predict more shocks, so it performs very well on flare events followed by shocks arriving at the Earth, but very badly on events without a shock arriving at the Earth. On the other hand, STOASF performs very well on events without shocks arriving, but relatively badly on events with shocks arriving. Actually, STOASEP, STAOF, and especially STOASF perform much better to reduce false alarm than STOA does. Low false alarm means high correct null. STOASF gets the highest correct null, 244, while STOA model missed the least shocks. STOA and STOASF get the worst and best success rate, respectively. It is noted that the number of observed events with shock, "hit(h) + miss(m)" is 229 and that the number of events without shock, "correct null(cn)+false alarm(fa)" is 356. In addition, the results of the χ^2 test for the four models are shown in Table 1. The p-values are all <0.05 which indicate a high level of significance. So we can have considerable confidence in these models.

[18] Furthermore, we adopt a set of forecast skill scores used by meteorological community [McKenna-Lawlor *et al.*, 2006] to test the performance of different methods. The forecast skill scores we use are (i) probability of detection, yes (POD_y); (ii) probability of detection, no (POD_n); (iii) false alarm ratio (FAR); (iv) ratio of number of events with shock forecast to that with shock detection (BIAS); (v) critical success index (CSI); (vi) true skill score (TSS), (vii) Heidke skill score (HSS); (viii) Gilbert skill score (GSS). Note that for scores POD_y, POD_n, CSI, TSS, HSS, and GSS, the higher scores are better, and for score FAR, a lower score is better, while for BIAS, a score nearer to 1 is better. For the detailed description of these scores, please refer to McKenna-Lawlor *et al.* [2006].

[19] The skill scores of the models with the 585 solar flare events in Solar Cycle 23 are listed in Table 2. POD_y represents the model's ability in forecasting the solar flare events with shocks arriving at the Earth, and POD_n represents the model's ability in forecasting the solar flare events without shocks arriving at the Earth. The POD_y and POD_n for STOA are 0.75 and 0.35, respectively. The small value of POD_n means there are too much false alarms. However, compared

with STOA, the new methods STOAF and STOASF's performance is slightly worse for POD_y but much better for POD_n. Notably, STOASF's POD_n is twice as large as STOA's. Furthermore, the BIAS of STOA is 1.76, and that of STOASF is 1.11 which is much closer to 1. While STOASEP and STOAF, get moderate BIAS (1.36 and 1.33, respectively). In addition, the two new methods all get much higher scores of TSS, HSS and GSS than STOA does. It is noted that the four models almost give the same root square of the ΔT , i.e., the root mean square of ΔT from STOA, STOASEP, STOAF and STOASF are 11.6, 11.5, 11.9 and 11.5 hours, respectively.

5. Conclusion and Discussion

[20] With the help of soft X-ray observations at L1, two new SAT prediction methods, STOAF and STOASF, are provided in this work. The two new methods need the observation of peak intensity of soft X-ray f during solar flare events, and the event duration τ , both of which can be derived from the temporal profiles of the GOES X-ray flux. Furthermore, E'_x , a simplified variable from the soft X-ray peak intensity and the duration time to approximately measure the energy released by a flare in soft X-ray, E'_x [Smith *et al.*, 1994], is used in the new methods. According to E'_x we divide the flare events into three types. Type I includes the events with small soft X-ray peak intensities or short durations which indicates the associated solar flare events are too weak to generate shocks or generate shocks that are not strong enough to arrive at L1. If the events belong to type I, no matter what the other conditions are, the method will always give a No prediction which means no shock will arrive at L1. On the contrary, the associated soft X-rays of the solar flare events belong to type III are with large soft X-ray energy, and it is believed that they would more likely generate shocks that could arrive at L1. So Yes predictions will be given no matter what other conditions are. The left events belong to type II that have moderate soft X-ray energy, then we use magnetoacoustic Mach number or the solar energetic particles to predict whether the shock will arrive at L1. The separation of the time-intensity space into regions could be done differently, but we think the way we do it here has physics meaning, and the values we choose in equation (1) give best prediction. We also tried different way, e.g., a straight line to separate region III, but could not get good result. In addition, similar as STOA, the two new methods need the initial coronal shock

velocity, the piston driving time, and the flare's location on the Sun. Furthermore, the solar wind velocity measured at 1 AU, or 400 km/s if it is not available, is needed. At last, STOASF also needs the SEP observations by ACE/EPAM.

[21] The performance of the two new methods, STOAF and STOASF, together with the two old models, STOA and STOASEP, are evaluated using the 585 solar flare events and their relative observations at L1 during the Solar Cycle 23. Compared with STOA, the two new methods get higher success rate, especially the STOASF model. In addition, the two new methods' scores of several standard meteorological skills (POD_n, FAR, BIAS, TSS, HSS and GSS) are much better than that of STOA. Therefore, it is shown that the soft X-ray energy could be used to improve SAT prediction models. However, since the soft X-ray energy and SEP flux are used to mainly reduce those events without shock arriving from forecast in the new methods, some events with shock arriving are missed. Therefore, the STOA model tends to predict shocks more often than the other three models, so its POD_v value is the highest. However, the STOASF has the ability to predict the correct null, or "all clear" forecast. To be able to reliably predict all clear periods is very important from the point of view of operational predictions. In addition, since all the models use the method of STOA to predict the arriving time of shocks, they get the similar root square of the ΔT . Compared with STOASEP, although STOAF model does not improve the SAT prediction, it uses observation data at L1 from different satellites/instrument, so the new method STOAF is still useful in case the data of one satellite is not available in real time.

[22] The physics-based 3D numerical models that start at the Sun [e.g., *S. T. Wu et al.*, 2006, 2011; *Feng et al.*, 2007, 2009, 2011] can simulate the magnetic structures in solar wind and the propagation of their disturbance. Although, with excessive computation resources requirements, the performance of these models in prediction of solar wind disturbance usually does not surpass that of other ones, it is essential for the space weather prediction that the quantitative physics-based 3D numerical simulation of solar wind is eventually used in practice.

[23] In the future, we will continue to study the improvement of other SAT prediction models instead of STOA with the help of soft X-ray energy and SEP measurement at 1 AU.

[24] **Acknowledgments.** The authors benefited from the soft X-ray flare data from the GOSE satellite provided by NOAA/NGDC and the ACE/EPAM high solar energetic electrons data provided by the ACE science data center. This work was supported partly by grants NNSFC 40921063, NNSFC 41125016, NNSFC 41074125, CMA grant GYHY201106011, and National High-tech R&D Program of China (863 Program) 2010AA122200.

[25] Philippa Browning thanks Murray Dryer and another reviewer for their assistance in evaluating this paper.

References

- Detman, T., Z. Smith, M. Dryer, C. D. Fry, C. N. Arge, and V. Pizzo (2006), A hybrid heliospheric modeling system: Background solar wind, *J. Geophys. Res.*, *111*, A07102, doi:10.1029/2005JA011430.
- Dryer, M. (1974), Interplanetary shock waves generated by solar flares, *Space Sci. Rev.*, *15*, 403–468.
- Dryer, M., and S. F. Smart (1984), Dynamical models of coronal transients and interplanetary disturbances, *Adv. Space Res.*, *4*, 291–301.
- Dulk, G. A., M. D. Altschuler, and S. F. Smerd (1971), Motion of type II radio burst disturbance in the coronal magnetic field, *Astrophys. Lett.*, *8*, 235.
- Feng, X. S., Y. F. Zhou, and S. T. Wu (2007), A novel numerical implementation for solar wind modeling by the modified conservation element/solution element method, *Astrophys. J.*, *655*, 1110–1126, doi:10.1086/510121.
- Feng, X. S., Y. Zhang, W. Sun, M. Dryer, C. D. Fry, and C. S. Deehr (2009), A practical database method for predicting arrivals of "average" interplanetary shocks at Earth, *J. Geophys. Res.*, *114*, A01101, doi:10.1029/2008JA013499.
- Feng, X. S., S. Zhang, C. Zhang, L. Yang, C. Jiang, and S. T. Wu (2011), A hybrid solar wind model of the CESE+HLL method with a Yin-Yang overset grid and an AMR grid, *Astrophys. J.*, *734*, 50.
- Fry, C. D., W. Sun, C. S. Deehr, M. Dryer, Z. Smith, S.-I. Akasofu, M. Tokumaru, and M. Kojima (2001), Improvements to the HAF solar wind model for space weather predictions, *J. Geophys. Res.*, *106*, 20,985–21,001.
- Fry, C. D., M. Dryer, Z. Smith, W. Sun, C. S. Deehr, and S.-I. Akasofu (2003), Forecasting solar wind structures and shock arrival times using an ensemble of models, *J. Geophys. Res.*, *108*(A2), 1070, doi:10.1029/2002JA009474.
- Gold, R. E., M. Krimigis, S. E. Hawkins, D. K. Haggerty, D. A. Lohr, E. Fiore, T. P. Armstrong, G. Holland, and L. J. Lanzerotti (1998), Electron and Alpha Monitor on the Advanced Composition Explorer spacecraft, *Space Sci. Rev.*, *86*, 541–562.
- Gopalswamy N., A. Lara, P. K. Manoharan, and R. A. Howard (2005), An empirical model to predict the 1-AU arrival of interplanetary shocks, *Adv. Space Res.*, *36*, 2289–2294.
- Lewis, D., and M. Dryer (1987), Shock-Time-of-Arrival model (STOA-87), NOAA/SEL contract report, U.S. Air Weather Serv., Scott Air Force Base, Ill.
- Manoharan, P. K., N. Gopalswamy, S. Yashiro, A. Lara, G. Michalek, and R. A. Howard (2004), Influence of coronal mass ejection interaction on propagation of interplanetary shocks, *J. Geophys. Res.*, *109*, A06109, doi:10.1029/2003JA010300.
- McKenna-Lawlor, S. M. P., M. Dryer, M. D. Kartalev, Z. Smith, C. D. Fry, W. Sun, C. S. Deehr, K. Kecskemety, and K. Kudela (2006), Near real-time predictions of the arrival at Earth of flare-related shocks during Solar Cycle 23, *J. Geophys. Res.*, *111*, A11103, doi:10.1029/2005JA011162.
- Odstreil, D., J. A. Linker, R. Lionello, Z. Mikic, P. Riley, V. J. Pizzo, and J. G. Luhmann (2002), Merging of coronal and heliospheric numerical two-dimensional MHD models, *J. Geophys. Res.*, *107*(A12), 1493, doi:10.1029/2002JA009334.
- Qin, G., M. Zhang, and H. K. Rassoul (2009), Prediction of the shock arrival time with SEP, *J. Geophys. Res.*, *111*, A09104, doi:10.1029/2009JA014332.
- Schwenn, R., A. D. Lago, E. Huttunen, and W. D. Gonzalez (2005), The association of coronal mass ejections with their effects near the Earth, *Ann. Geophys.*, *23*, 1033–1059.
- Smart, D. F., and M. A. Shea (1985), A simplified model for timing the arrival of solar flare-initiated shocks, *J. Geophys. Res.*, *90*, 183–190.
- Smart, D. F., M. A. Shea, W. R. Barron, and M. Dryer (1984), A simplified technique for estimating the arrival time of solar flare-initiated shocks, in *STIP Workshop on Solar/Interplanetary Intervals, August 4–6, 1982, Maynooth, Ireland*, edited by M. A. Shea et al., pp. 139–156, Bookcrafters, Inc., Chelsea, Mich.
- Smart, D. F., M. A. Shea, M. Dryer, A. Quintana, L. C. Gentile, and A. A. Bathurst (1986), Estimating the arrival time of solar flare-initiated shocks by considering them to be blast waves riding over the solar wind, in *Solar-Terrestrial Predictions: Proceedings of a Workshop at Meudon, France, June 18–22, 1984*, edited by P. A. Simon, G. Heckman, and M. A. Shea, pp. 471–481, U.S. Gov. Print. Off., Washington, D. C.
- Smerd, S. F. (1970), Radio evidence for the propagation of magnetohydrodynamic waves along curved paths in the solar corona, *Proc. Astron. Soc. Aust.*, *1*, 305.
- Smith, Z., and M. Dryer (1990), MHD study of temporal and spatial evolution of simulated interplanetary shocks in the ecliptic plane within 1 AU, *Solar Phys.*, *129*, 387–405.
- Smith, Z., M. Dryer, and M. Armstrong (1994), Can soft X-ray be used as a proxy for total energy injected by a flare into the interplanetary medium?, in *Solar Coronal Structures: Proceedings of the 144th IAU Colloquium*, edited by V. Rusin, P. Heinzel, and J.-C. Vial, pp. 267–270, VEDA Publ., Bratislava.
- Smith, Z., M. Dryer, E. Ort, and W. Murtagh (2000), Performance of interplanetary shock prediction models STOA and ISPM, *J. Atmos. Terr. Phys.*, *62*, 1265–1274.
- Smith, Z. K., T. R. Detman, M. Dryer, C. D. Fry, C. C. Wu, and W. Sun (2004), A verification method for space weather forecasting models using solar data to predict arrivals of interplanetary shocks at Earth, *IEEE Trans. Plasma Sci.*, *32*(4), 1498–1505, doi:10.1109/TPS.2004.832509.
- Smith, Z. K., M. Dryer, S. M. P. McKenna-Lawlor, C. D. Fry, C. S. Deehr, and W. Sun (2009a), Operational validation of HAFv2's predictions

- of interplanetary shock arrivals at Earth: Declining phase of Solar Cycle 23, *J. Geophys. Res.*, *114*, A05106, doi:10.1029/2008JA013836.
- Smith, Z. K., R. Steenburgh, C. D. Fry, and M. Dryer (2009b), Operational validation of HAFv2's predictions of interplanetary shock arrivals at Earth: Declining phase of Solar Cycle 23, *J. Geophys. Res.*, *114*, A05106, doi:10.1029/2008JA013836.
- Stewart, R. T., K. V. Sheridan, and K. Kai (1970), Evidence of type II and moving type IV solar bursts excited by a common shock wave, *Proc. Astron. Soc. Aust.*, *1*, 313.
- Wu, C. C., X. S. Feng, S. T. Wu, M. Dryer, and C. D. Fry (2006), Effects of the interaction and evolution of interplanetary shocks on "background" solar wind speeds, *J. Geophys. Res.*, *111*, A12104, doi:10.1029/2006JA011615.
- Wu, S. T., A. H. Wang, Y. Liu, and J. T. Hoeksema (2006), Data-driven magnetohydrodynamic model for active region evolution, *Astrophys. J.*, *652*, 800–811.
- Wu, S. T., A. H. Wang, C. C. Wu, F. Hill, I. G. Hernández, X. S. Feng, and M. Dryer (2011), A global solar wind model based on surface measurements of magnetic field and transverse velocity from GONG, in *5th International Conference of Numerical Modeling of Space Plasma Flows (ASTRONUM 2010)*, edited by N. Pogorelov, *ASP Conf. Ser.*, *444*, 143.